

---

ETD Archive

---

2011

## FEA Analysis of Novel Design of Cylindrical Roller Bearing

Prasanna Subbarao Bhamidipati  
*Cleveland State University*

Follow this and additional works at: <https://engagedscholarship.csuohio.edu/etdarchive>



Part of the [Mechanical Engineering Commons](#)

**How does access to this work benefit you? Let us know!**

---

### Recommended Citation

Bhamidipati, Prasanna Subbarao, "FEA Analysis of Novel Design of Cylindrical Roller Bearing" (2011). *ETD Archive*. 629.

<https://engagedscholarship.csuohio.edu/etdarchive/629>

This Thesis is brought to you for free and open access by EngagedScholarship@CSU. It has been accepted for inclusion in ETD Archive by an authorized administrator of EngagedScholarship@CSU. For more information, please contact [library.es@csuohio.edu](mailto:library.es@csuohio.edu).

FEA ANALYSIS OF NOVEL DESIGN OF CYLINDRICAL ROLLER  
BEARING

PRASANNA SUBBARAO BHAMIDIPATI

Bachelor of Science in Mechanical engineering

R.C.E, affiliated to Jawaharlal Nehru technological university

Hyderabad, India

May, 2006

submitted in partial fulfillment of requirements for the degree

MASTER OF SCIENCE IN MECHANICAL ENGINEERING

at the

CLEVELAND STATE UNIVERSITY

December 2011

This thesis has been approved  
for the Department of **MECHANICAL ENGINEERING**

And the College of Graduate Studies by

---

Thesis Committee Chairperson, Dr. Majid Rashidi

---

Department, Date

---

Dr. Rama S.R. Gorla

---

Department, Date

---

Dr. Asuquo Ebiana

---

Department, Date

## **DEDICATED TO.....**

To my parent and my brother who made my life possible and encouraged me in all the stages in my life

**“Sharma Bhamidipati”  
“Naga Lakshmi Bhamidipati”  
“Sai Uday Bhamidipati”**

To my uncle’s family who made me believe that “I can do it” and for the continues support to my family

**“Subrahmanyam V.V.R.S and family”**

To my fiancée for her continuous support and understanding

**“ Apoorva Balantrapu”**

To entire teaching staff of Mechanical engineering department at Cleveland state university for all support

**“C.S.U -Mechanical Engineering  
Department ”**

## ACKNOWLEDGEMENT

First, I would like to express my sincere gratitude to my advisor **Dr. Majid Rashidi** for his guidance, support and patience throughout this work. I have benefited a lot from his knowledge, insight and commitment towards helping his students and I would like to thank for all his guidance in my study. This would have been not possible without **Dr. Majid Rashidi** support and help.

I also would like to thank Dr. Rama S.R. Gorla, Dr. Asuquo Ebiana for being a part of thesis committee and for taking time to review my thesis.

I want to take this opportunity to thank entire department of Mechanical Engineering at Cleveland State University for all the support and special thanks to Dr. William Atherton M.E, chairman for all valuable suggestions.

On top of all, I owe a particular debt of gratitude and appreciation to my family for their consistent encouragement and advice through my life.

# FEA ANALYSIS OF NOVEL DESIGN OF CYLINDRICAL ROLLER BEARING

PRASANNA SUBBARAO BHAMIDIPATI

## ABSTRACT

This work presents a finite element stress analysis of a novel design of cylindrical roller. The focus of this study is to create a uniform contact-stress distribution along the length of the roller and to recommend a roller bearing design which is easier to fabricate.

The new design relies on creating symmetric cylindrical cavities at both ends of a roller. The cavity is concentric with the main body of the roller. The new roller design reduces overall mass of the typical assembly with helps to improve bearing life and its overall performance.

The FEA results published herein shows that new roller design eliminates a roller edge stresses which is conventionally achieved by the crowning of the roller ends. This work shows that the maximum contact stress of typical unmodified end is reduced from 1380 M pa to 1220 M pa for a typical end modified of 3 mm deep and 12.50 diameters (Table V). Also, the new roller design allows an overall mass reduction of the roller by 12% (Table V).

## TABLE OF CONTENTS

ABSTRACT.....	v
LIST OF TABLES.....	viii
LIST OF FIGURES.....	x
LIST OF SYMBOLS.....	xi
CHAPTER	
I.INTRODUCTION & BACKGROUND.....	1
1.1    Bearing failure modes.....	1
1.2    Previous research.....	2
1.3    Expected contribution.....	3
1.4    Structure of the thesis.....	4
II.CLOSE FORM FORMULATION OF CONTACT STRESS FOR LINE- CONTACT CONFORMITY.....	5
2.1    Hertz formulation of line contact conformity..	5
2.2    Contact stress behavior at the boundaries of cylinders pressed together.....	7
2.2.1    The two contacting surface of same length.....	7
2.2.2    Raceway is extended beyond the roller surface.....	8
2.2.3    Crowned roller cylinder.....	9
III.PROPOSED ROLLER DESIGN.....	12
3.1    Proposed roller profiles by H.Hertz and G. Lundberg.....	12

3.2	Alternative roller end configuration .....	13
3.3	Finite element modeling and design parameters.....	14
3.4	3-D FEA results comparison with Hertz's formulation.....	15
IV.FINITE ELEMENT ANALYSIS (FEA) RESULTS AND CONCLUSION		18
4.1	Double-ended hollow roller concept FEA results review.....	19
4.2	Summary and conclusion.....	28
REFERENCE.....		29
APPENDIX -A.....		31
A.1	Importance of meshing to minimize mathematical errors.....	35



## LIST OF TABLES

Table	page
I     Hertz's mathematical problem-Properties and dimensional parameters.....	15
II    Hertz's theoretical mathematical formulation.....	16
III   Iteration 1: Design Parameter & contact pressure plots for $(r^*, d^*) = (12.50 \text{ mm}, 1 \text{ mm})$ .....	21
IV   Iteration 2: Design Parameter & contact pressure plots for $(r^*, d^*) = (12.50 \text{ mm}, 2 \text{ mm})$ .....	22
V    Iteration 3: Design Parameter & contact pressure plots for $(r^*, d^*) = (12.50 \text{ mm}, 3 \text{ mm})$ .....	23
VI   Iteration 4: Design Parameter & contact pressure plots for $(r^*, d^*) = (12.50 \text{ mm}, 5 \text{ mm})$ .....	24
VII   Iteration 5: Design Parameter & contact pressure plots for $(r^*, d^*) = (12.50 \text{ mm}, 7.5 \text{ mm})$ .....	25
VIII   Iteration 6: Design Parameter & contact pressure plots for $(r^*, d^*) = (12.50 \text{ mm}, 10 \text{ mm})$ .....	26
IX    Iteration 7: Design Parameter & contact pressure plots for $(r^*, d^*) = (12.50 \text{ mm}, 12.5 \text{ mm})$ .....	27

X	Solidworks simulation –GUI setting.....	32
XI	Units systems.....	32
XII	Material assignment.....	32
XIII	Restraints and loads .....	33
XIV	Contact pairs .....	34
XV	Mesh information.....	35
XVI	Bearing assembly mating assumption.....	36

## LIST OF FIGURES

Figure		Page
1	Contact of elastic bodies.....	6
2	Contact of two cylindrical bodies.....	6
3	Contact pressure of two contacting surfaces of same length.....	8
4	Contact pressure of race-way extended beyond the roller surface.....	9
5	Roller with both ends “crowned”.....	10
6	Contact pressure of crowned roller cylinder.....	10
7	Proposed roller design.....	14
8	FEA contact stress plot for Stress distribution along inner race-line of contact.....	16
9	Different roller profiles and the corresponding contact-stress distributions [5].....	17
10	Schematic view of the roller studied in this work.....	20

## LIST OF SYMBOLS

Symbol	description
$p$	Force per unit length
$a$	Width
$U_{z1,z2}$	Displacement
$z_1,z_2$	Distance
$s_1,s_2$	Function of “x”
$E$	Young’s modulus
$R$	Radius of curvature
$p_o$	Maximum contact pressure
$r$	Radius
$W_z$	Heaviest roller load
$r^*$	Cavity diameter
$d^*$	Cavity depth

# **CHAPTER I**

## **INTRODUCTION & BACKGROUND**

### **1.1 Bearing failure modes:**

When a bearing is properly designed, manufactured, installed, and maintained, then the natural cause of bearing failure is typically the fatigue life of its rolling elements and races. The environment within which the bearing operates also determines the bearing life.

The contact stresses developed in the rolling elements and races of a typical bearing is cyclic in nature. This in turn will result in a potential fatigue failure for these elements. The fatigue life a bearing is influenced by the operating speed, load conditions, bearing material, clearance of the mating parts, contact surface geometry, and the environment in which the bearing operates.

The fatigue failure modes, mentioned above, could be categorized according the following list:

- Rolling element surface fatigue
- Common wears of the interacting surfaces (races and rollers)
- Cross-sectional cracking and fretting.

The cross-sectional cracking and fretting could be caused by unusual and/or abnormal operating conditions that were not considered during the bearing design. Excessive “hoop-stresses”, caused by centrifugal forces, could lead to race-way fractures [Zaretsky and Loe, 1987].

## **1.2 Previous research:**

It has been a common practice for many decades to utilize cylindrical shaped roller bearing elements in machinery in order to evenly distribute the bearing load across the line contact between the rollers and race-ways. However, designing a bearing such that a uniform contact stress distribution is resulted along the contact lines of a roller bearing is highly unrealistic. This difficulty stems from the fact that the two ends of a typical roller act as stress-concentration zones, causing the contact stresses to have spikes at the roller end points. The conventional method of rectifying this undesirable condition is to modify the geometric configuration of the ends of the roller in a way that a sharp or abrupt transition from the contact line to the cross-section of the roller is avoided. This geometric modification is called “crowning” of the roller. Figure 9, show contrasts between an unmodified and a crowned roller respectively, with their corresponding contact stress distributions.

A substantial amount of research work has been done to study structural integrity and behavior of cylindrical rolling elements, which have been crucial parts of a typical bearing from contact stress point of view. Many researchers and designers have developed various analytical, numerical, and experimental techniques in order to predict and improve contact stress distributions along the contact line of rolling element bearings. For, example Dareing and Zimovsly [1964] proposed analytical techniques in order to computationally predict the contact stress distribution along the contact line of a rolling element that is not crowned. Hardnett ,Kannel [1981], and Heydave and Goohar [1979] included nonlinear behavior of the contacting surfaces under stress and came up with an analytical solution to better predict the stress distribution at the contact line.

With the advent of various advanced FEA codes, and fast computational hardware, the inherent difficulties of solving nonlinear FEA problem have been addressed and resolved to a great extent.

In this research, Solidworks Simulation was used as the FEA solver importing parametric models from Solidworks.

### **1.3 Expected contribution:**

Empirical and real-world applications of roller element bearings have shown that if the crowned geometry is not accurate, the uniform stress distribution may not be realized. In other words, eliminating the contact stress spikes at the ends of a typical roller becomes highly sensitive to manufacturing tolerances and accuracies. Thus the bearing life and its performance largely depend upon the manufacturing accuracy of the rollers.

In this thesis an innovative alternative approach for elimination or minimizing the stress spikes at the ends of a typical roller is studied. This alternative roller manufacturing approach will require less effort, especially in terms of keeping close tolerances. Chapter 3 of this document describes this alternative method.

#### **1.4 Structure of the thesis:**

The structure of this thesis is as follows. In Chapter 2, Illustrates Hertz's [2] close-form formulation for solving contact stress and Response of different cross-sectional roller end conditions under load is described.

In chapter 3, proposed roller design and design parameter is described and 3-D Finite element analysis (FEA) simulation of a roller-inner/outer race contact stress is summarized briefly and its results are compared with Hertz's [2] in-line contact formulations. In chapter 4, FEA for proposed roller design, the procedure and results are reported. Further, research contributions and future research topics are summarized.

Finally, Appendix 1 is documented which describes geometrical, parametric settings and all the assumptions considered for this research work.



## **CHAPTER II**

### **CLOSE-FORM FORMULATION OF CONTACT STRESS FOR LINE-CONTACT CONFORMITY**

#### **2.1 Hertz Formulation for Line-Contact Conformity:**

Figure 1 and 2 shows two cylindrical bodies with their longitudinal axes parallel. The cylinders are pressed by a force of  $p$  per unit length as shown in Figure 1. The contact area between the two bodies is a rectangle of width  $2a$  having a length equal to that of the cylinders.

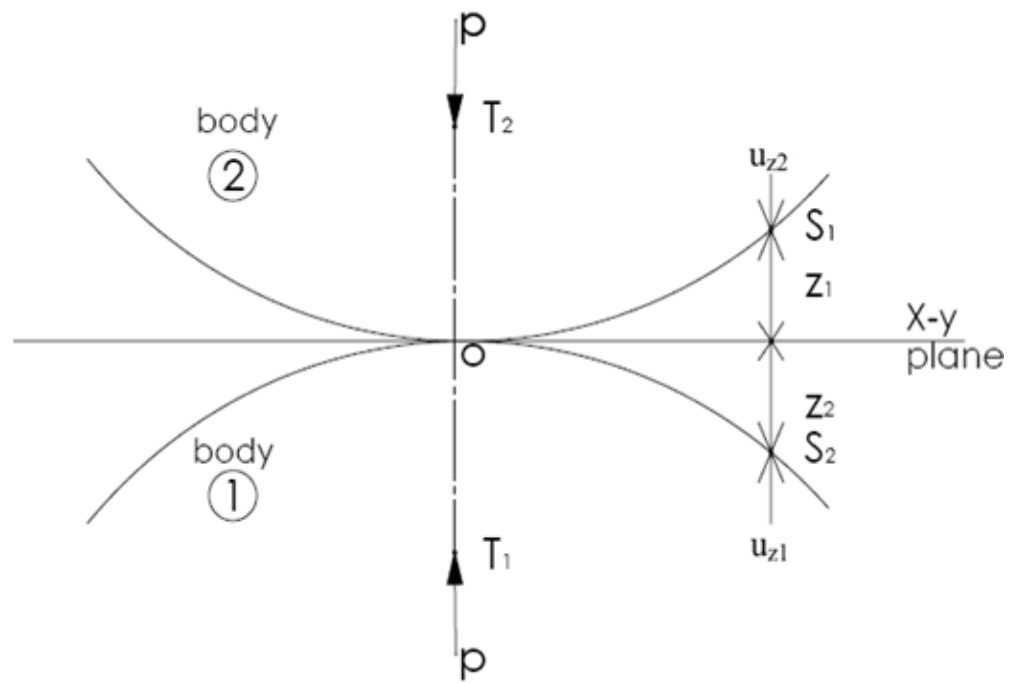


Figure 1: Contact of elastic bodies

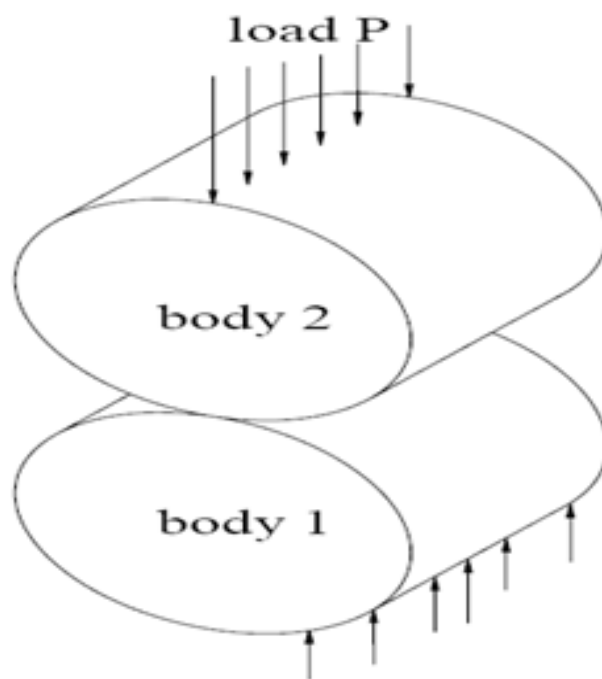


Figure 2: Contact of two cylindrical bodies

Therefore for the consistent pressure distribution, the pressure should sum-up to

$$p = \frac{\Pi a^2 E^*}{4R} \quad (2.1) \text{ and } a^2 = \frac{4pR}{\Pi E^*},$$

$$p(x) = \frac{2p}{\Pi a^2} (a^2 - x^2)^{\frac{1}{2}}$$

And  $p(x)$  falls to zero at the edge of the contact.

The maximum pressure is

$$p_o = \left( \frac{pE^*}{\Pi R} \right)^{\frac{1}{2}} \quad (2.2)$$

## **2.2 Contact stress behavior at the boundaries of cylinders pressed together:**

The contact stress at the end points of two cylinders pressed together exhibits stress concentration behavior. In order to avoid these stress concentration points in a typical roller bearing, the axial profile of the roller is modified from a straight cylindrical shape to a barrel shape configuration. This geometric modification results in eliminating or minimizing the stress concentration at the ends of the rollers. The different possible modified end conditions that yield a fairly uniform contact stress in discussed below.

### **2.2.1 The two contacting surfaces of same length:**

Both roller and race-way are of the same length and come to end at the same cross-sectional plane. On cross-sections away from the ends, an axial compressive stress exists to maintain the condition of plane strain. At the free ends this compressive stress reduces

in value, allowing the solids to expand slightly in the axial direction and thereby reducing the contact pressure at the end as shown in Figure 3. An estimate of the reduction in the pressure at the end of the roller may be obtained by assuming that the end of cylinder is under a state of plane stress.

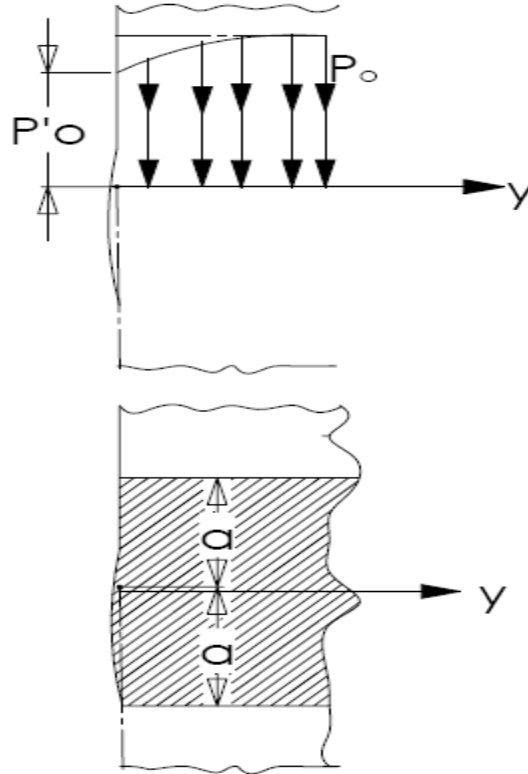


Figure 3: Contact pressure of two contacting surfaces of same length

### 2.2.2 Race-way is extended beyond the roller surface:

The Roller has a square edge with race-way extending beyond the end of the roller.

Under this condition there is a sharp stress concentration at the end of the roller as shown in Figure 4.

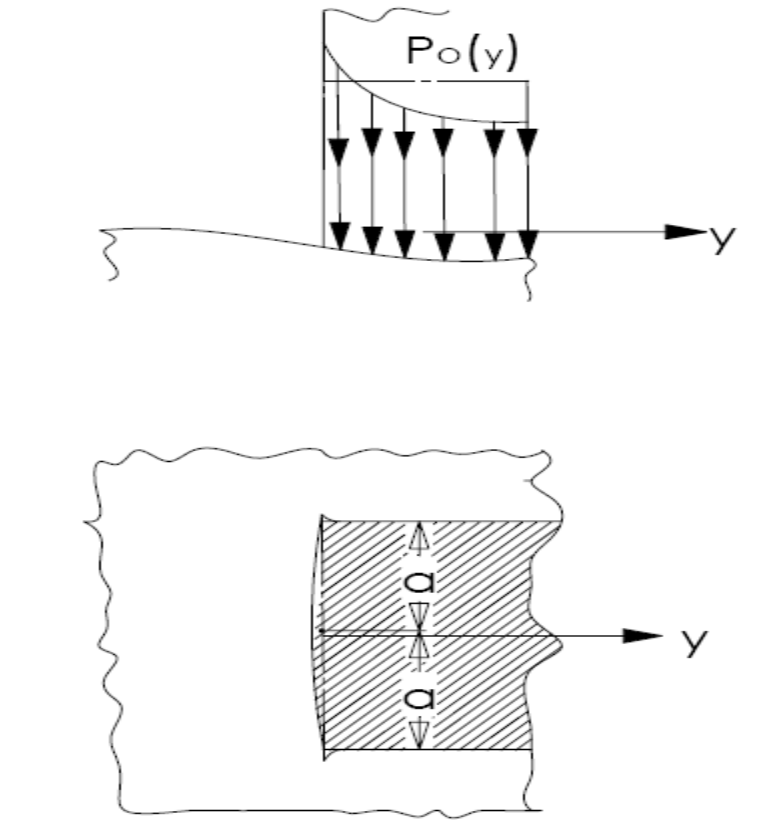


Figure 4: Contact pressure of race-way extended beyond the roller surface

### 2.2.3 Crowned roller cylinder:

In order to eliminate or reduce the stress concentration shown in Figure 4, it is customary to modify (removing material) from the ends of a roller. A well known roller-end modification is called crowning. Figure 5, shows a schematic view of a roller with its both ends “crowned”.

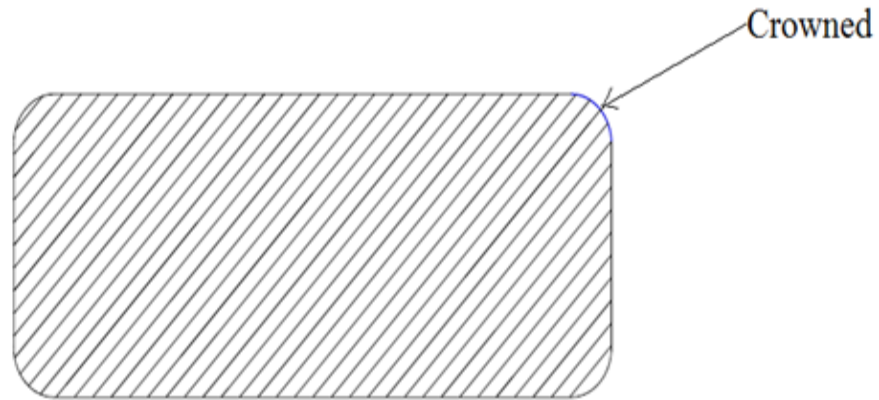


Figure 5: Roller with both ends “Crowned”

The crowned roller configuration shown in figure 5 is a preferred shape of a typical cylindrical roller. The roller has a radius of “ $r$ ”, this geometric configuration results in reduction of the edge-stresses. A “dog bone” shape contact shown in Figure 5, is developed after “crowning” the roller ends.

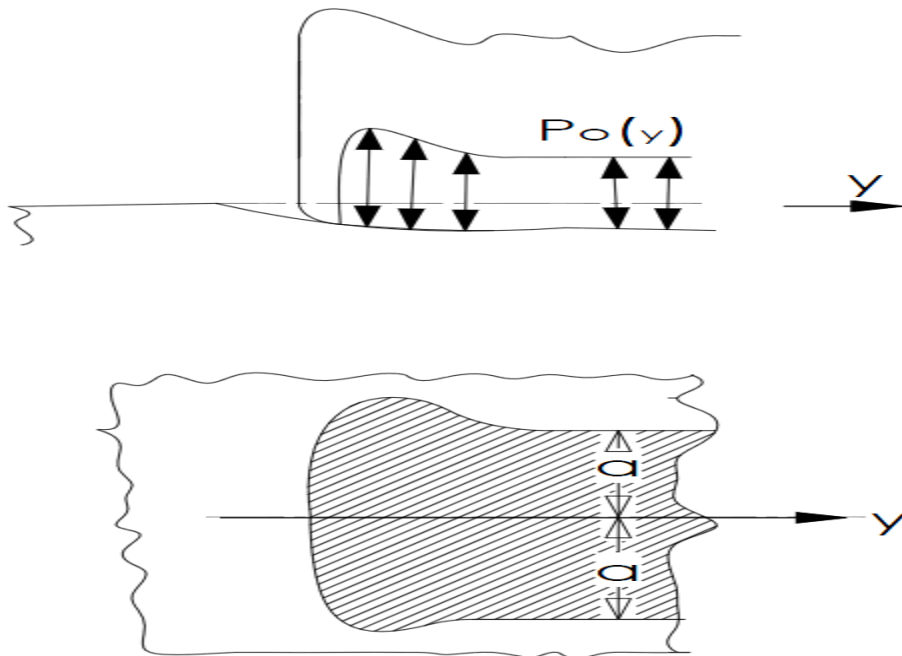


Figure 6: Contact pressure of crowned roller cylinder

In next chapter, an alternative modification for the geometric configuration of a typical roller is proposed. Subsequently a 3-D FEA simulation of a roller-inner/outer race contact stress is discussed briefly.

## **CHAPTER III**

### **PROPOSED ROLLER DESIGN**

#### **3.1 Proposed roller profiles by H.Hertz and G.Lundberg:**

During the past few decades the design of cylindrical roller bearings has been significantly improved. These improvements are mainly achieved by advancement in bearing steel materials and geometric design improvements. The design enchantments are mostly focused on contact stress reduction at the bearing rolling contact regions. It has been shown [1] that bearing life is inversely proportional to the stress raised to the ninth power or even higher. For this reason significant efforts have been put in for solving extensive range of contact problems [2-4].

It was recognized from theoretical formulation proposed by H.Hertz [8] and G. Lundberg theory [1], as well as from laboratory tests [5], that changes by a few micrometers to the



profile of the roller has a significant effect on the bearing life. A concrete theoretical relationship between roller profile and bearing life was never known; even to this date such theoretical relationships have not been successfully established. The optimum geometry of the roller profile modifications has been established more or less by trial-and-error or by empirical approaches.

The circular arc profile, commonly known as crowning, resulted from the Hertzian theory, whereas the cylindrically crowned profiles is a straight central portion with crowned edges which was based on the Lundbery theory [1].

Use of these two methods of profile modifications resulted in considerable progress to identify relative accuracy of edge profiles necessary to sustain uniform contact stress distribution across the roller length.

However, theoretical relationships between a roller profile and bearing load-carrying capacity for a given operating conditions have not been successfully established. After many years of research, logarithmic [5] profile for cylindrical roller bearing was proposed but the logarithmic profiles was mostly confined to the research and engineering applications due to precise manufacturing requirement.

### **3.2 Alternative roller end configuration:**

This thesis examines a novel roller design as shown in Figure 7, which offers many advantages when compared to Logarithmic, Crowning, or cylindrical-crowned rollers profiles.

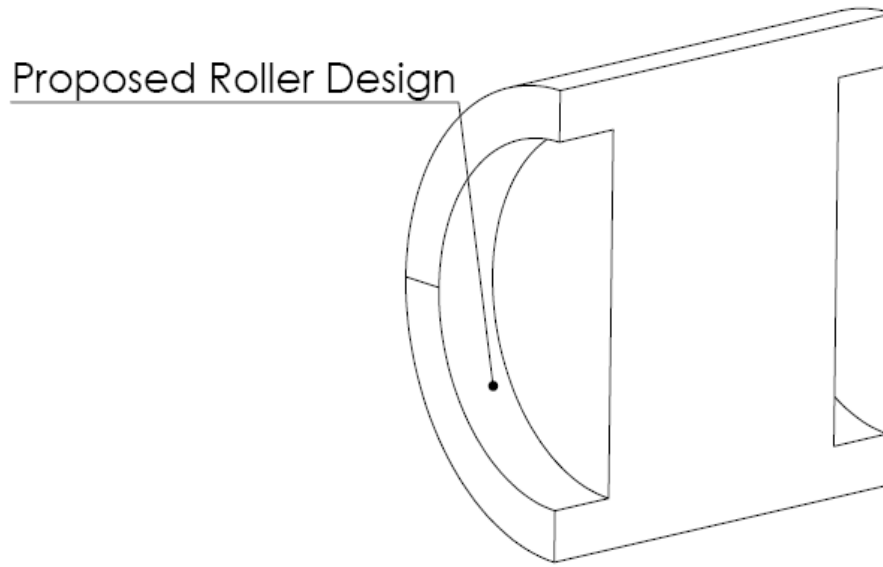


Figure 7: Proposed roller design

The research conducted in this thesis also focused on designs which are more responsive to varying bearing loads and which has lesser manufacturing restrictions. Also the design concept studied in this work will reduce overall mass of the bearing, thus reducing the centrifugal force acting on the outer-race, which could also contribute to an increase in the bearing life.

### **3.3 Finite Element Modeling and Design Parameters:**

Finite Element analysis was done to study the contact stresses developed in a typical roller as shown in Figure 9 (a). Solidworks simulation Software is used to simulate to realistic boundary and load conditions as described in Appendix-A.

The rest of this chapter describes FEA study of non-crowned roller bearing profile under load and then results are compared with Hertz formulation (Equation 2.2).

For the roller shown in the Figure 9 (a), the roller radius of  $\phi 32$  mm is chosen. The mechanical properties of bearing material are assigned with a young's Modulus of  $2.09 \times 10^5$  MPa, Poisson's ratio of 0.33 and refer Table I for more information.

Appendix-A describes more details on the mathematical problem formulation, physical parameters in modeling, material property, constraints definition, loading distribution definition, meshing control technique ,contact pairs definitions ,contact set definitions, and the solver definitions used for FEA analysis.

Table I

<b>Hertz's Mathematical problem-Properties and dimensional parameters</b>	
Roller diameter	$\phi 32$ mm
Roller length	31 mm
Outer race diameter	$\phi 232$ mm
Inner race diameter	$\phi 158$ mm
Type of material	Bearing steel
Young's Modulus - inner race and roller	$2.09E + 05$ Mpa
Corresponding poison's ratio	0.33
Radial load	100000 N

### 3.4 3-D FEA results comparison with Hertz's formulation:

The rest of this chapter is about a comparison of the FEA results with Hertz theory of contact mechanics [2] both applied to a typical roller for the purpose of validation of the results predicted by the FEA. In Table II the results predicted by the Hertz model [5] are

compared with FEA results, which show that FEA Results matches with Hertz theoretical calculation with 3.2% Percentage error.

Table II

Hertz's Theory Mathematical formulation	
w(N)	100000
Rx(meters)	0.013
l(meters)	0.031
Hertz contact stress	2.94E+09 Mpa
FEA result	2.85E+09 Mpa
percentage error	3.2

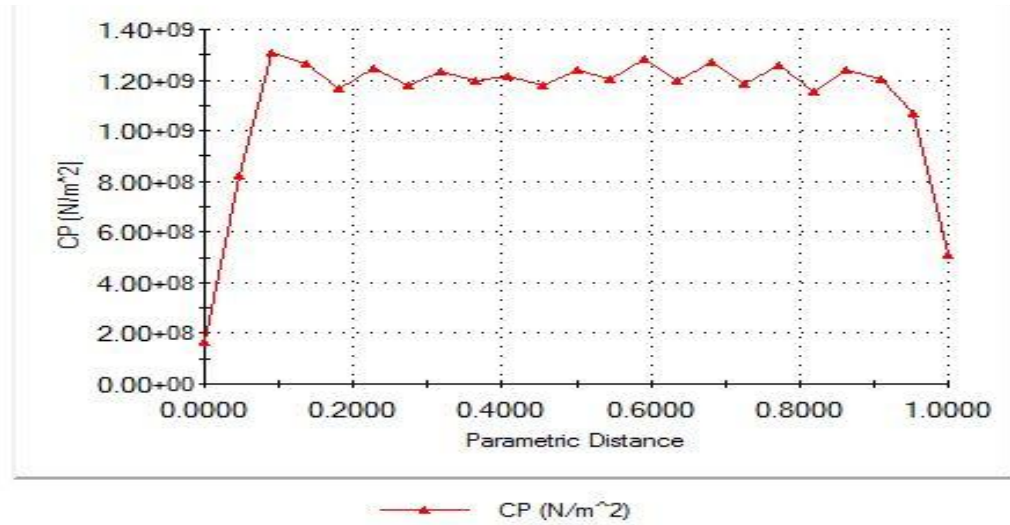


Figure 8: FEA contact stress plot for Stress distribution along roller line of contact

### Contact stress distribution of different roller profiles

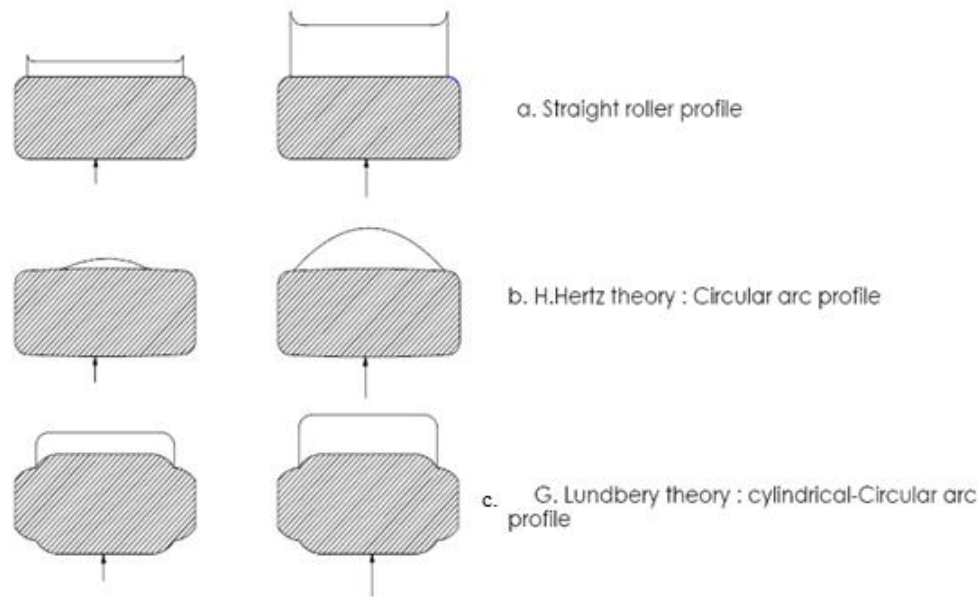


Figure 9: Different roller profiles and the corresponding contact-stress distributions [5].

As described in appendix-A Hertz's FEA analysis section A.7, cross-section of roller and race-ways are in the same end-plane and under load, a compressive stress exists away the roller ends. The FEA results as shown in the figure 8 shows a similar compressive stress allowing roller to expansion at ends which results in reduction of the contact stresses at the roller ends[8].

The next chapter describes the results of a FEA performed on the alternative roller design that is shown in Figure 7.

## **CHAPTER IV**

### **FINITE ELEMENT ANALYSIS, RESULTS AND CONCLUSION**

The previous efforts to establish a uniform contact-stress distribution along the length of a typical cylindrical roller was mainly focused on changing the roller profile and utilizing advanced bearing steels materials. This work however takes a different approach by studying of a novel roller end configuration that results in reduced roller stiffness at its ends in the radial direction.

This research explore a new roller shape to provide a relatively uniform contact stress distribution along the length of a roller by reducing the contact stiffness of the roller in the radial direction of the roller's transverse cross-section. The approach relies on a novel double-ended hollow roller design which has straight profile with end-cavities at the two ends of the roller. Figure 10 shows a schematic view of the roller studied in this work.

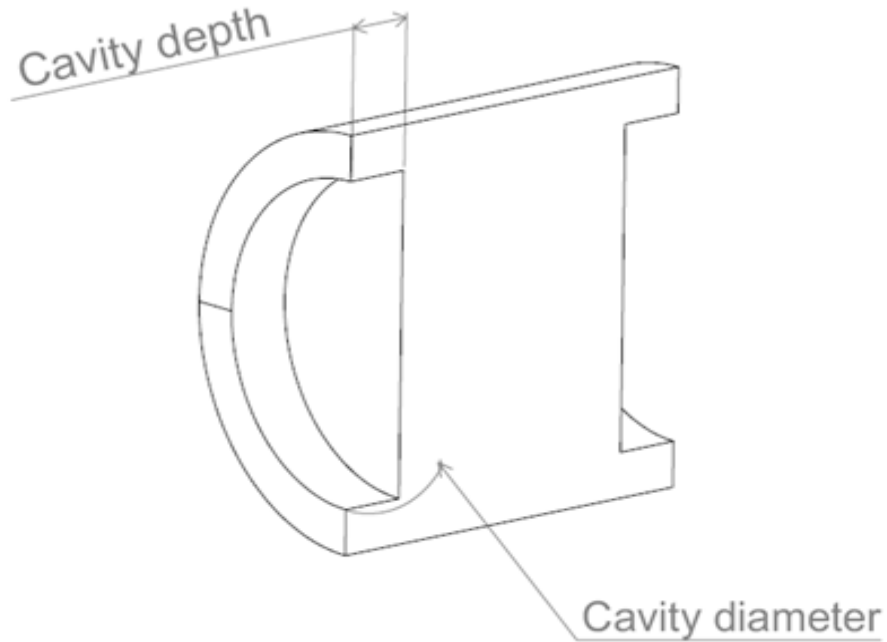


Figure 10: Schematic view of the roller studied in this work

As shown in Figure 10, the double-ended hollow roller has a cavity diameter of  $r^*$  and a cavity depth of  $d^*$ .

The double-ended hollow roller has the characteristic of deflecting at two ends of the roller in response to radial loading. This results in a reduction of the contact stress at the roller's ends. In other words, double-ended hollow roller design establishes an elastic behavior of roller ends and allows deflection of the roller ends in the radial direction which is along the direction of the applied contact load. In addition to these benefits, this design concept will reduce the mass of a bearing, reducing the inertia effects acting on the outer raceway, which directly improves overall bearing life span.

#### **4.1 Double-ended hollow roller concept FEA results review:**

As discussed in Chapter 3, Finite Element analysis simulations for the proposed Double-ended hollow roller concept was done by a combination of solidworks and

Solidworks simulation software's. Appendix-A of this thesis contains the following details on the physical parameters employed in modeling:

- Material properties
- Constraints definition
- Loading distribution
- Meshing control technique
- Contact pair definition
- Contact set definitions, and
- Solver definition

This work examines the influence of varying the two parameters  $r^*$  and  $d^*$  on the compressive stress distribution along the length of the roller.

Appendix-A contains the finite element analysis formulation that was employed to determine optimum values for  $r^*$  and  $d^*$ .

After running several FEA runs an optimum cavity diameter of  $r^* = 12.50$  mm was obtained. Further FEA simulations were performed with fixed Cavity diameter of 12.50 mm with varying cavity depth of  $d^*$ .

To mimic realistic bearing working conditions, an off-set of 0.5 mm was postulate between roller plane and the inner/outer raceway planes. Here, no crowing radius was used for roller design. Instead, the roller ends was simulated to have a configuration as that of shown in Figure 10. A radial line load was applied along the inner diameter of inner race. Refer to Appendix-A for more details about load distribution parameters.

The remaining of this chapter illustrates the FEA simulation of a typical roller bearing with design variables and the corresponding results are presented showing the compressive stress distribution along the roller length.



The first FEA simulation was created by selecting the cavity depth of 1mm and cavity diameter of 12.50 mm

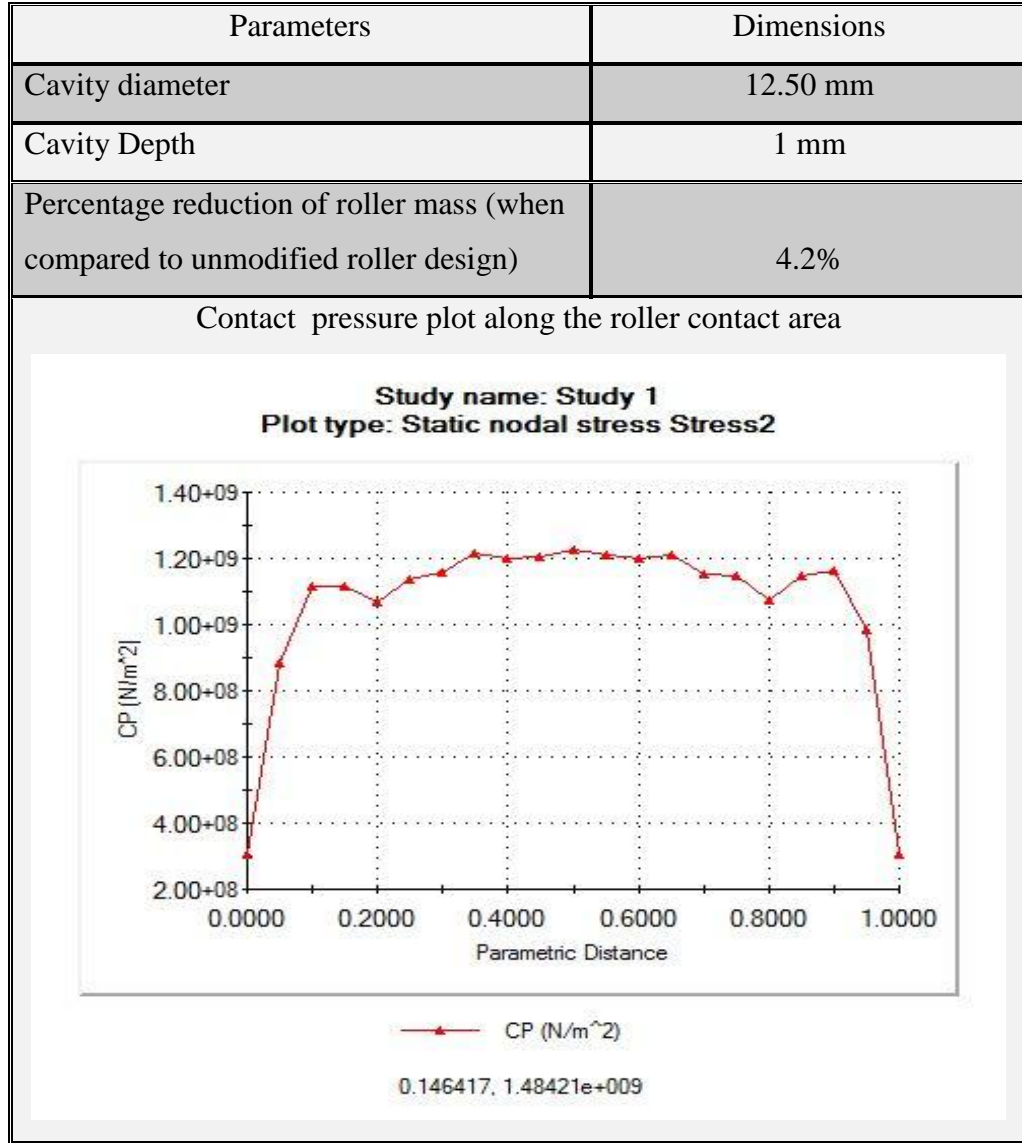


Table III: Design Parameter & contact pressure plot for  $(r^*, d^*) = (12.50\text{mm}, 1\text{mm})$

The second configuration was performed with cavity depth of 2 mm and 12.50 mm cavity diameter. Table IV contains the results of configuration 2

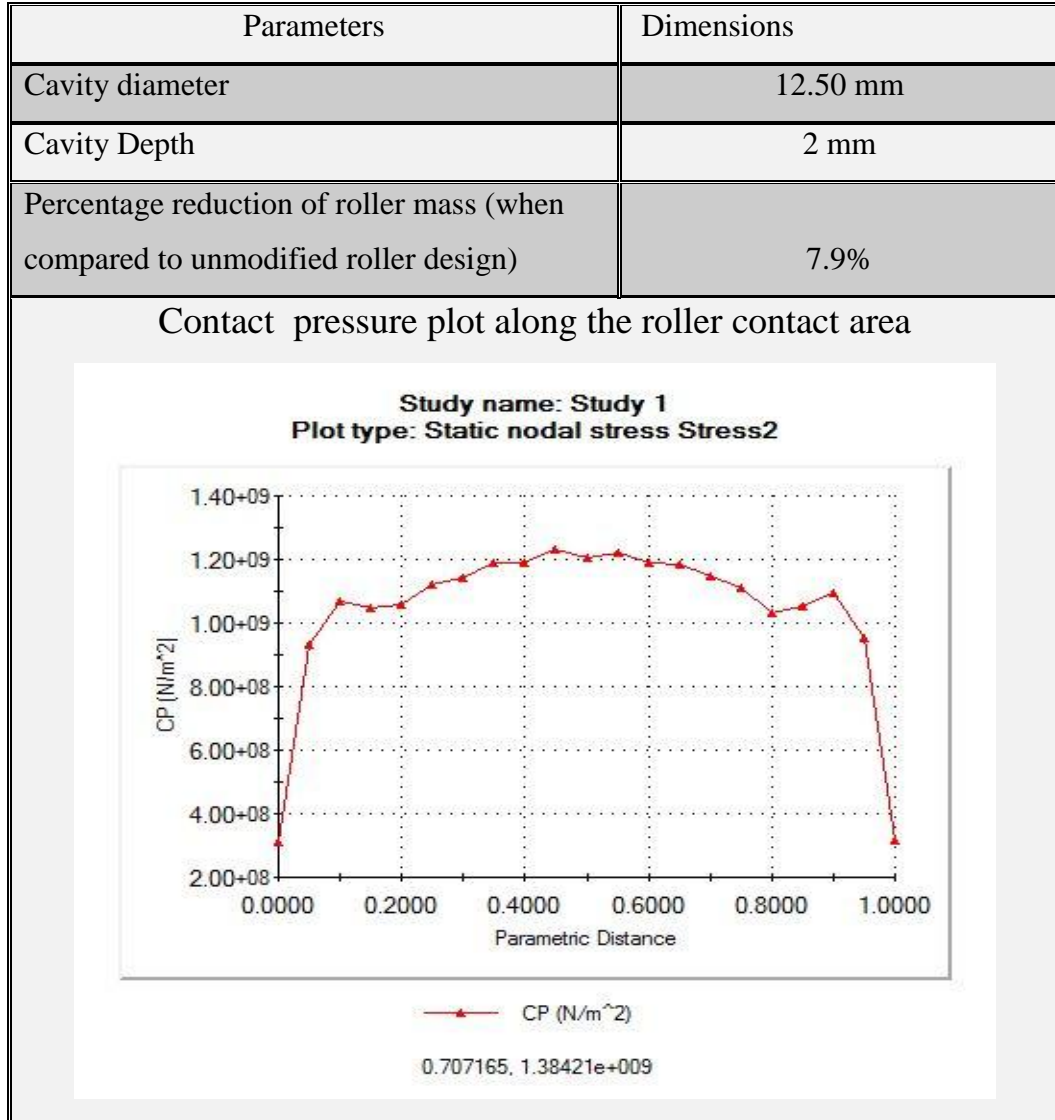


Table IV: Design Parameter & contact pressure plot for  $(r^*, d^*) = (12.50 \text{ mm}, 2 \text{ mm})$

The third configuration was performed with a cavity depth of 3 mm and 12.50 mm cavity diameter. The result of this configuration is summarized in Table V and it also shows FEA results of unmodified roller design. The results shows that the maximum contact stress of typical unmodified end is reduced from 1380 M pa to 1220 M pa for a typical end modified of 3 mm deep and 12.50 diameters. Also, the new roller design allows an overall mass reduction of the roller by 12%.

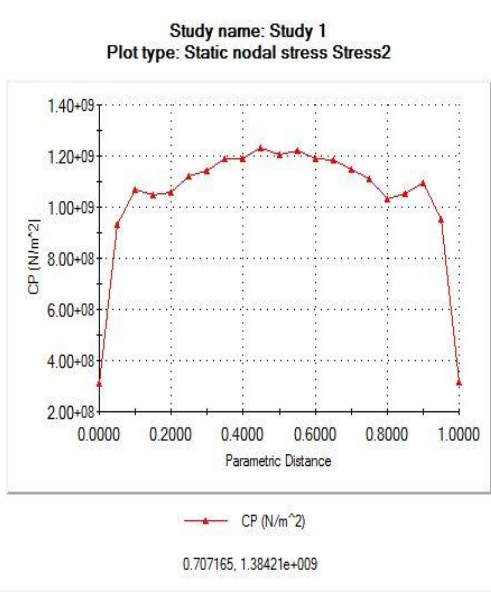
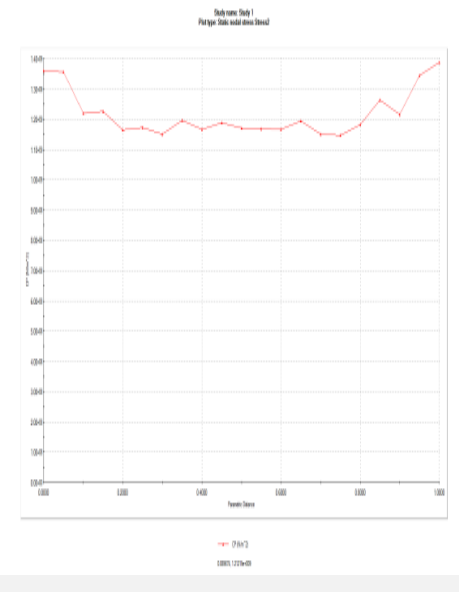
Parameters	Dimensions
Cavity diameter	12.50 mm
Cavity Depth	3 mm
Percentage reduction of roller mass (when compared to unmodified roller design)	12.0%
<p>Contact pressure plot along the roller contact area: The maximum contact stress of typical end modified of 3 mm deep and 12.50 diameters is 1380 M pa.</p>  <p>The plot shows contact pressure (CP) in N/m² on the y-axis (ranging from 2.00e+08 to 1.40e+09) against parametric distance on the x-axis (ranging from 0.0000 to 1.0000). The curve starts at approximately 3.00e+08, rises to a peak of about 1.25e+09 at a distance of 0.5, and then falls back to approximately 3.00e+08. A legend indicates 'CP (N/m²)' with a red line and diamond markers. Below the plot, the values '0.707165, 1.38421e+009' are displayed.</p>	<p>Contact pressure plot for unmodified roller: The maximum contact stress of typical unmodified end is 1220 M pa.</p>  <p>The plot shows contact pressure (CP) in N/m² on the y-axis (ranging from 1.00e+08 to 1.60e+09) against parametric distance on the x-axis (ranging from 0.0000 to 1.0000). The curve starts at approximately 1.50e+09, drops to about 1.20e+09, and then fluctuates between 1.20e+09 and 1.40e+09. A legend indicates 'CP (N/m²)' with a red line and diamond markers. Below the plot, the values '0.707165, 1.38421e+009' are displayed.</p>

Table V: Design Parameter & contact pressure plots for  $(r^*, d^*) = (12.50 \text{ mm}, 3 \text{ mm})$

The fourth configuration was performed with a cavity depth of 5 mm and 12.50 mm cavity diameter and refer table VI for contact stress plots along roller.

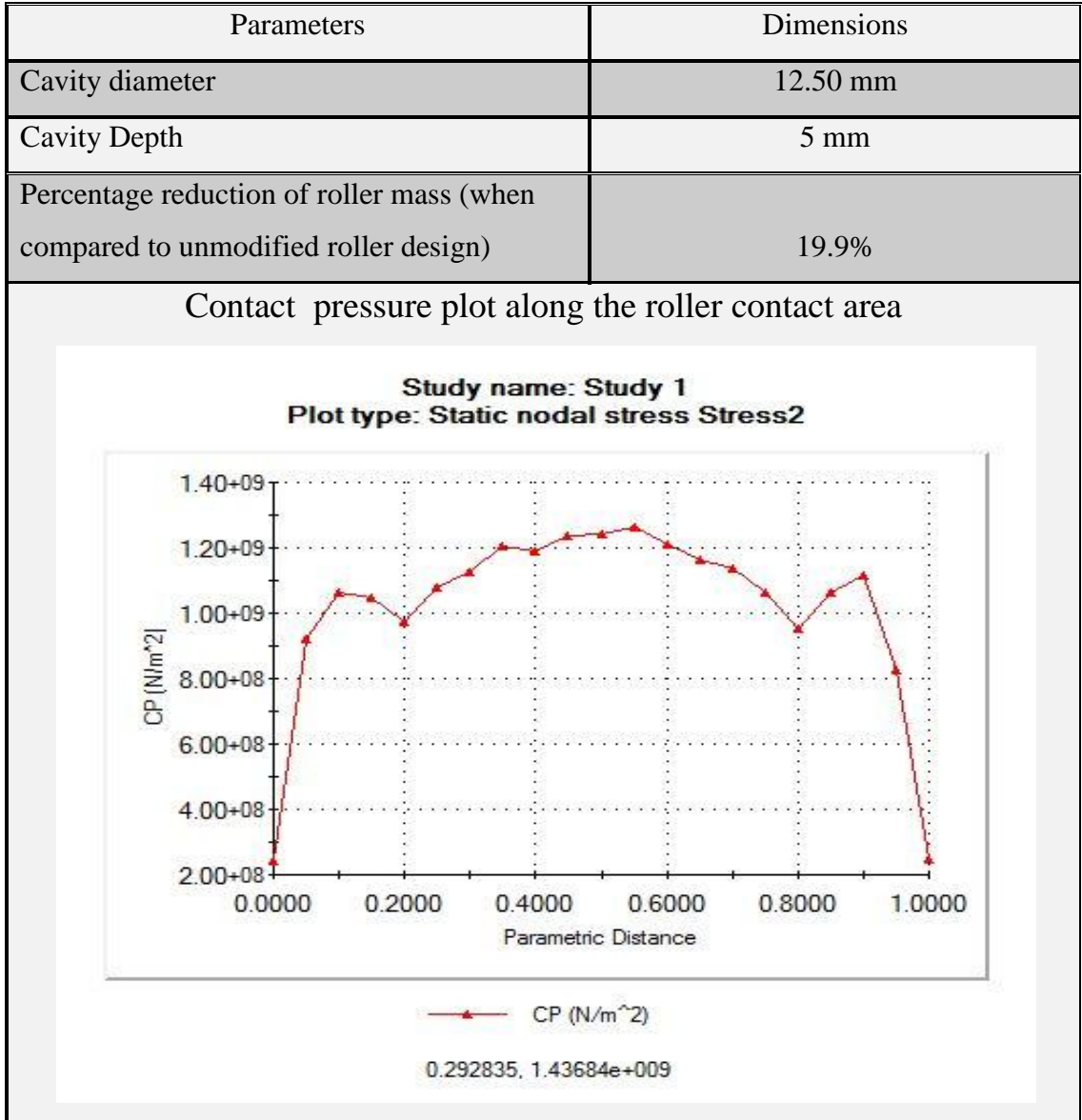


Table VI: Design Parameter & contact pressure plots for  $(r^*, d^*) = (12.50 \text{ mm}, 5 \text{ mm})$

The fifth configuration was performed with cavity depth of 7.5 mm with 12.50 mm cavity diameter and refer table VII, for contact stress plots along roller and inner race.

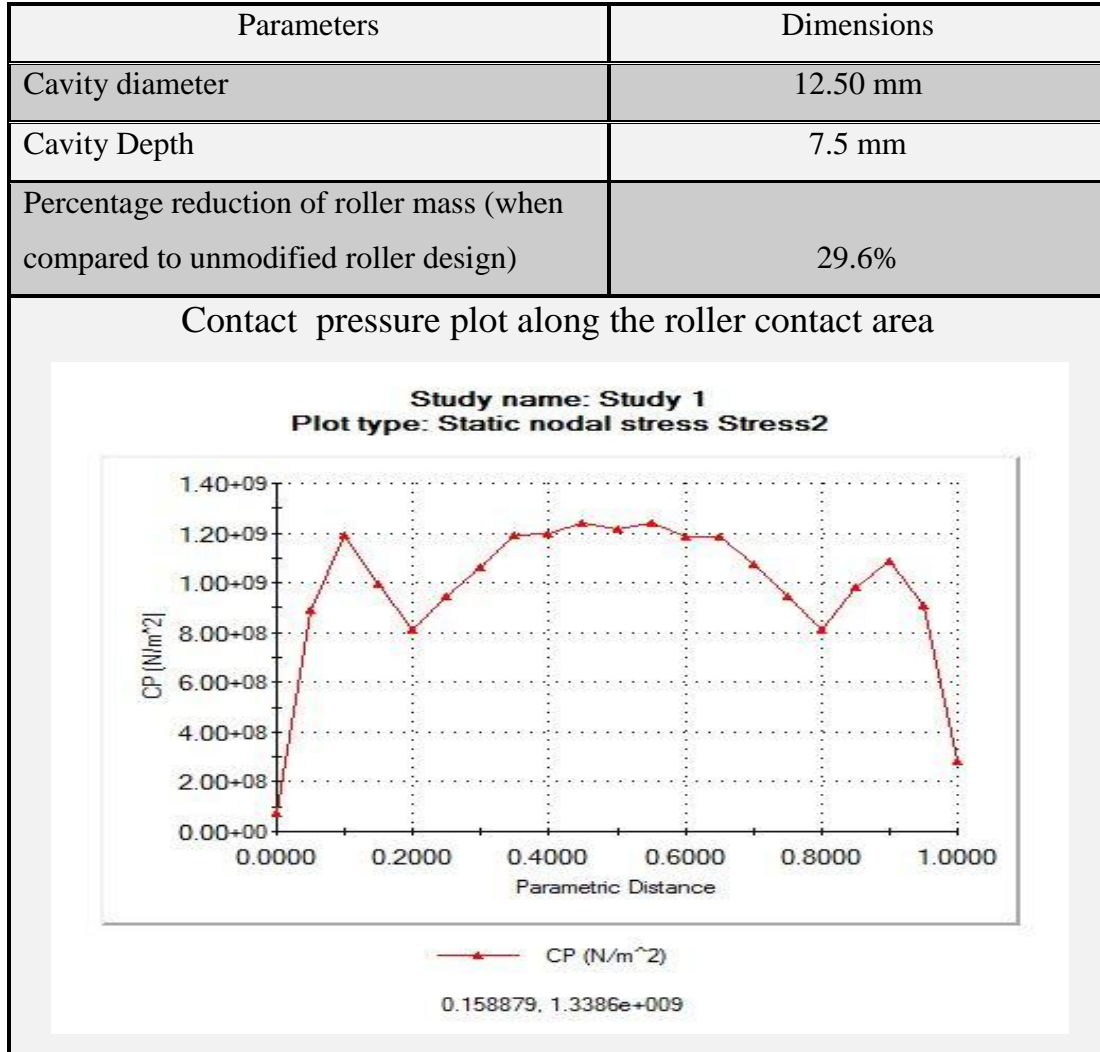
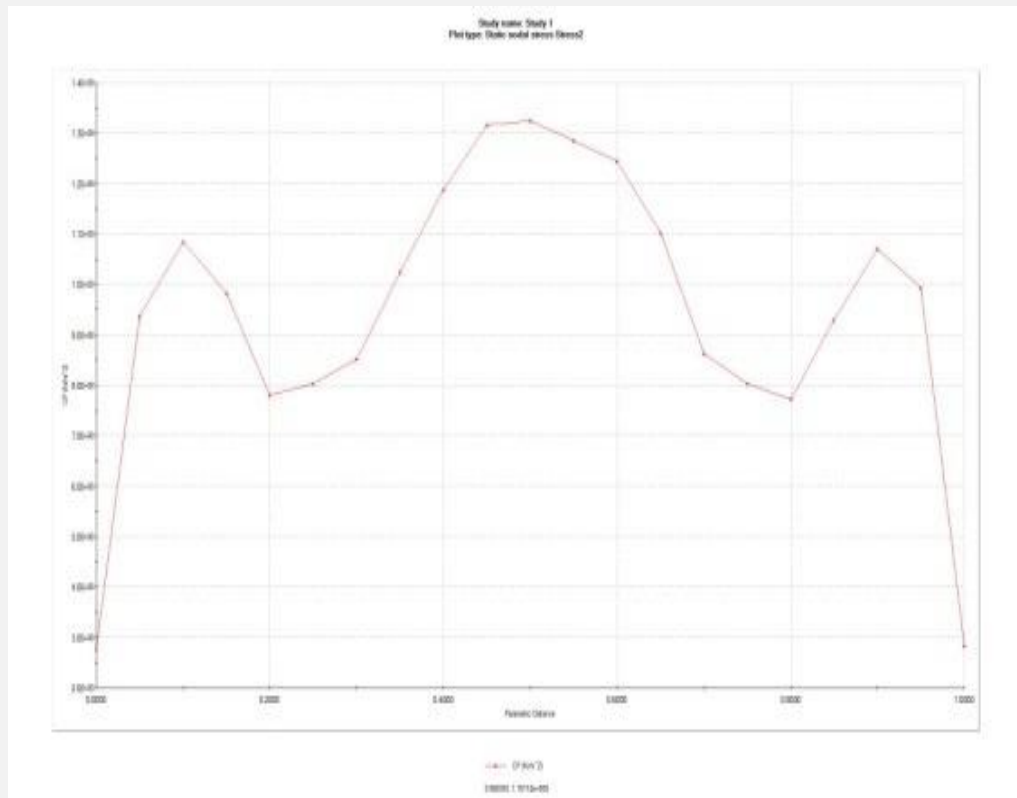


Table VII: Design Parameter & contact pressure plots for  $(r^*, d^*) = (12.50 \text{ mm}, 7.5 \text{ mm})$

The sixth configuration was performed with a cavity depth of 10 mm and 12.50 mm cavity diameter and refer table VIII for contact stress plots along roller and inner race.

Parameters	Dimensions
Cavity diameter	12.50 mm
Cavity Depth	10 mm
Percentage reduction of roller mass (when compared to unmodified roller design)	39.4%

Contact pressure plot along the roller contact area

Table VIII: Design Parameter & contact pressure plots for  $(r^*, d^*) = (12.50 \text{ mm}, 10 \text{ mm})$

The seventh configuration was performed with a cavity depth of 12.50 mm and 12.50 mm cavity diameter. The results are shown in Table IX

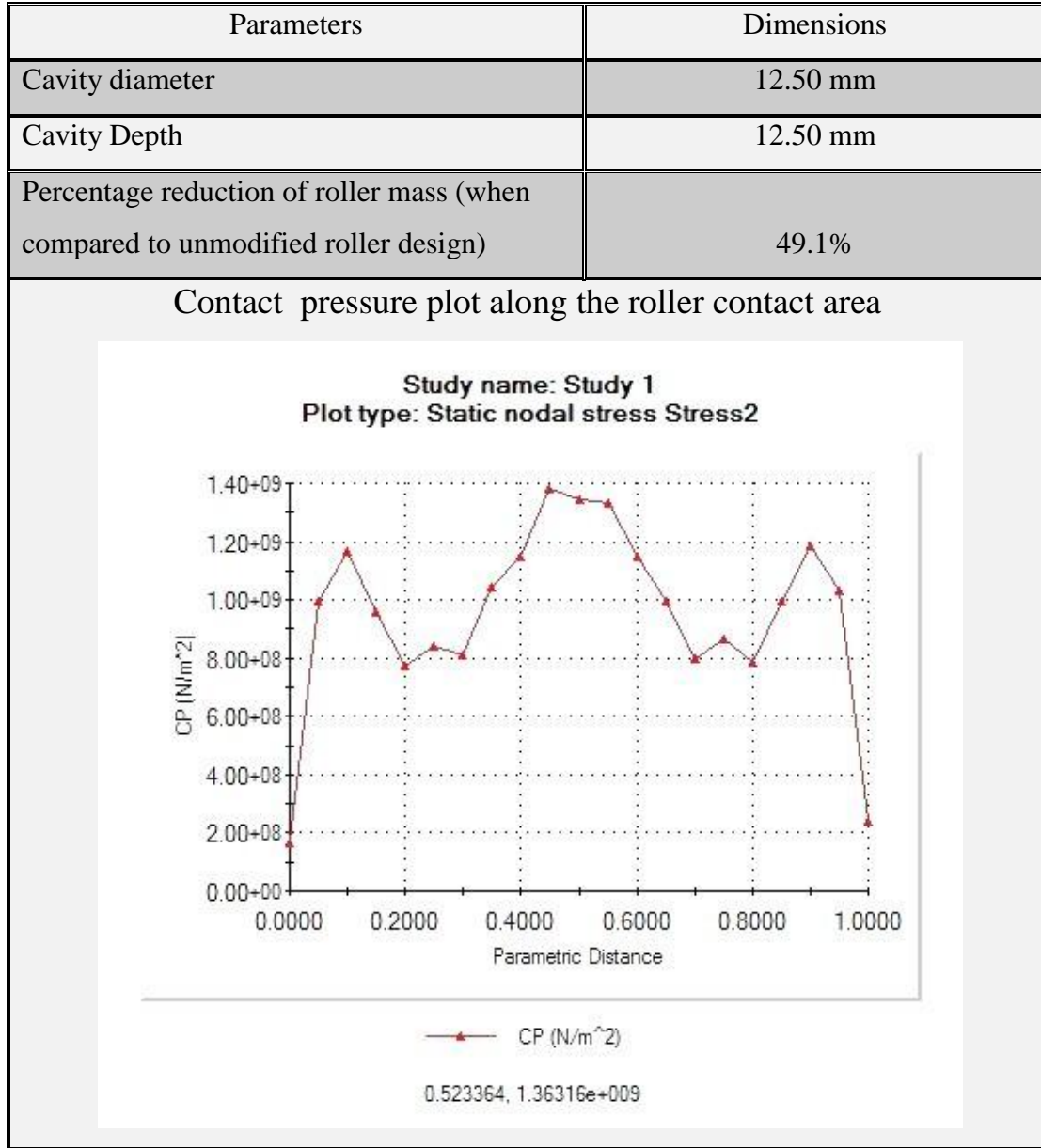


Table IX: Design Parameter & contact pressure plots for  $(r^*, d^*) = (12.50 \text{ mm}, 12.50 \text{ mm})$

## 4.2 Summary and conclusion:

The double-ended hollow roller presented in this thesis is mainly focused on studying a roller design which can develop uniform contact-stress distributions by eliminating any edge stress and also recommend a roller bearing design which is easier to fabricate.

As shown in Table V-configuration 3, the maximum contact stress of typical unmodified end is reduced from 1380 M pa to 1220 M pa by modifying the roller design with a cavity depth of 3 mm and cavity diameter of 12.50 mm. Also this work presents a roller design which has a lower manufacturing difficulty to fabricate when compared to conventional roller with crowned ends. This alternative roller design also reduces the over-all mass of the bearing assembly which in turn improves bearing life and its overall performance.

As illustrated in the above FEA configurations, with variations in the cavity depth  $d^*$ , the roller is relaxed to deflect due to the hollow cavity at the ends of the roller when subject to a compressive contact load, which in turn results in the reduction in contact stress distribution at both ends of the roller.



## REFERENCES

1. G.Lundberg, A. Palmgren, “Dynamic capacity of the rolling bearings”, Acta Polytechnica Mechanical Engineering series, Vol.1 No.1,Royal Swedish Academy of Engineering Sciences, Stockholm, Sweden,1947.
2. Hertz, H., “Miscellaneous papers- on the contact of elastic solids”, translation by Jones,D.E , Macmillan and Co, Ltd., London,1898.
3. Harris, T.A, “The effect of misalignment on the fatigue life of cylindrical roller bearing having crowned roller members”, ASME Journal of Lubrication Technology, Vol.91,Apr 1969,pp 294-300.
4. Liu,J.Y., “The effect of misalignment on the life of high-speed cylindrical roller bearings” ASME Journal of Lubrication Technology, Vol.93, NO.1,Jan 1971,pp 60-68.
5. H.Reusner, “The logarithmic roller profile-The key to superior performance of cylindrical and taper bearing”, Ball Bearing Journal, 230(1987) 2-10.
6. S.H,Ju, T.L Horng,K.C Cha, “Comparison of contact pressures of crowned rollers ”in proceedings of the institution of mechanical engineering Part 1,Journal of Eng. Tribology ,214 ,2000,pp147-156
7. SolidWorks® Simulation® software
8. K.L Johnson, “Contact Mechanics”, Cambridge, London 1985.

9. Anthony C. Fischer-Cripps, “Introduction to contact mechanics”

## **APPENDIX-A**

This section is gives complete over-view of geometrical, parametric setting utilized for this research work and describes all the assumptions that are consider while performing the research work and design parameters that used.

Lastly, this section also gives complete details of different analysis modules characteristics used in this research work

- Load and Restraints properties
- Meshing control techniques
- Contact set's selections and properties

Table X: Solidworks Simulation –GUI setting

Analysis type	Static
Mesh Type:	Solid Mesh
Solver type	FFEPlus
In plane Effect:	Off
Soft Spring:	On
Friction:	Off
Ignore clearance for surface contact	Off
Use Adaptive Method:	Off

Table XI: Units system:

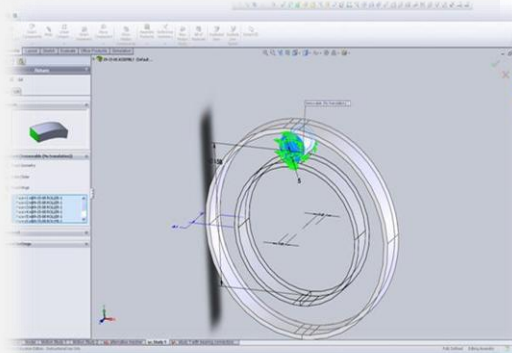
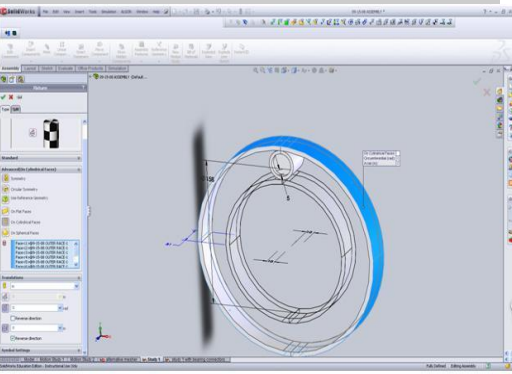
Unit system:	S.I system
Length/Displacement	meters
Temperature	Fahrenheit
Stress/Pressure	N/m <sup>2</sup>

Table XII: Material assignment

Material name	Bearing steel
Description: body name	Roller, inner race & outer race.
Material Source:	Design tree -Material GUI
Material Model Type:	Linear Elastic Isotropic
Default Failure Criterion:	Max von Mises Stress

Table XIII: Restraints and load

Restraints

Restraint name	Selection set	Description
Restraint-1	on 8 Face(s) immovable (no translation) on the roller	
Restraint-2	on 8 Face(s) with zero displacement along circumferential and axial directions on the outer race.	

Load:

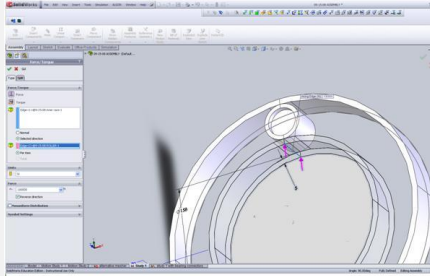
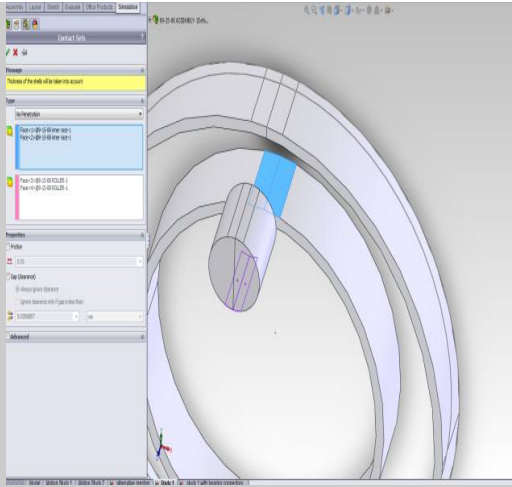
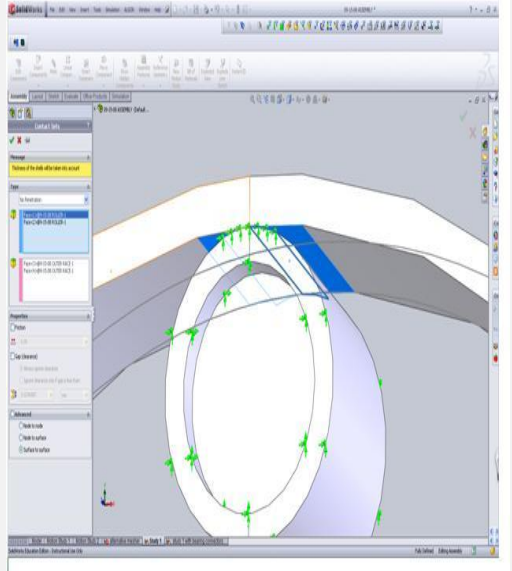
Load name	Selection set	Loading type	Description
Force-1	100 KN radial load is applied	Sequential Loading	

Table XIV: Contact pairs:

Contact set	Type	Description
<p>Contact Set-1</p> <p>Contact state: Touching faces - Free</p>	<p>No Penetration - contact pair between selected entities-</p> <p>Inner race surface to roller outer surface</p> <p>Source surface : O.D of inner race</p> <p>Target surface: Roller</p>	
<p>Contact Set-2</p> <p>Contact state: Touching faces - Free</p>	<p>No Penetration - contact pair between selected entities(blue colored surfaces)-outer race surface to roller outer surface</p> <p>Source surface: Roller Target surface: I.D of outer surface.</p>	

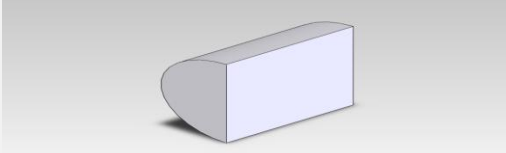
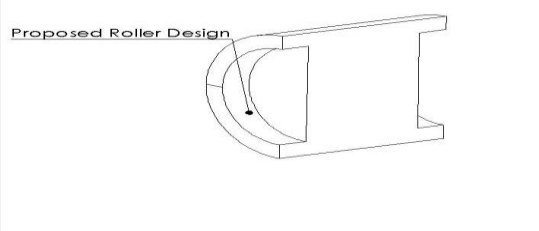
### A.1 Importance of meshing to minimize mathematical errors:

An FEA simulation always has some scope for mathematical error due to different types of contact. In a contact pairs, contact can only occur between nodes and the contact nodes can be discrete distance apart. So, the most accurate approximation for radius of the area of contact 'r' would be the average radial coordinates of the last node that has contacted and the next one that is not in contact. Since contact pressure involves a  $1/r^2$  term and the strain of the bodies in contact depend directly on r, any error in the estimation of the radius of contact is cubed [9]. Therefore, a large number of nodes are to be used in FEA simulation in order to minimize computational errors.

Table XV: Mesh Information

Mesh Type:	Solid Mesh
Jacobian Check:	At Nodes
Element Size:	3 mm
Tolerance:	0.15 mm
Quality:	High
Number of elements:	53946
Number of nodes:	92795

Table XVI: Bearing Assembly mating assumptions

Hertz's Formulation design parameters	Deep-double ended hollow bearing design
Cross-section's of roller and race-ways are in the same end-plane without any off-set	Cross-section's of the roller and race-ways are mated with 0.5 mm off-set
Roller, Race-ways are of same length- 31mm	Roller length of 30 mm and race-ways width of 31 mm
Non-crowning bearing roller design is analyzed	Proposed design as shown in Chapter 4 is analyzed
	
Dry contact (No friction) of rolling elements is assumed for the FEA simulations	Dry contact (No friction) of rolling elements is assumed for the FEA simulations
To simplify the complexity, a static cylindrical roller bearing is analyzed and to reduce FEA simulation run time, single roller was analyzed under load and no cage supports are incorporated in FEA simulations	To simplify the complexity, a static cylindrical roller bearing is analyzed and to reduce FEA simulation run time, single roller was analyzed under load and no cage supports are incorporated in FEA simulations
Magnitude of radial load or (Basic static load rating) is 100 KN	Magnitude of radial load or (Basic static load rating) is 100 KN